Towards Massive Ray-Based Simulations of mmWave Small Cells on Open Urban Maps

Dmitrii Solomitckii†, Margarita Gapeyenko†, Sebastian S. Szyszkowicz⋆,
Sergey Andreev†, Halim Yanikomeroglu⋆, and Yevgeni Koucheryavy†
†W.I.N.T.E.R. Group, Tampere University of Technology, Tampere, Finland
⋆BCWS Centre, Carleton University, Ottawa, Canada.

***Abstract*—Utilization of extremely high frequency (EHF) bands, known as millimeter-wave (mmWave) frequencies, requires a dense deployment of wireless small cells in order to provide continuous coverage for served users. At the same time, to be able to collect a sufficient amount of statistical data for constructing further analytical EHF models, a significant number of various landscape maps in different scenarios has to be considered. This paper develops a shoot-and-bounce based methodology capable of characterizing the mmWave propagation in open-space urban conditions. In particular, our methodology aims to capture a large number of small cells within accurate, real city maps, named here massive simulations. Hence, our contribution is to provide a suitable tool that is able to handle massive ray-based simulations within a reasonable time frame. In particular, we demonstrate that a shift from simulating 3D to evaluating 2D environments significantly reduces computation time while only slightly decreases the resulting modeling accuracy. In addition, we show that the corresponding performance degradation might potentially be improved by utilizing a two-ray model.**

***Index Terms*—Dense urban deployments; mmWave small cells; massive ray-based simulations.**

I. Introduction and Background

The increase in traffic demand and the growing needs of users in terms of throughput and latency require an introduction of emerging concepts as part of the fifth-generation (5G) mobile networks. The extremely high frequency (EHF) band is a promising candidate to support many key requirements of such future wireless communication systems. Making larger bandwidths available, the so-called millimeter-wave (mmWave) systems operating in the EHF band are expected to eventually provide around several Gbps of data rate [1], [2].

In addition to its benefits, mmWave system operation also poses unprecedented challenges. One of these is completely new channel characteristics that were not applicable in lower frequency bands. Due to the different nature of millimeter waves, one of the potential difficulties is considerable blockage caused by smaller objects [3], [4]. In addition, diffuse scattering will need to be accounted for in mmWave systems. All of the above brings the need to comprehensively analyze the propagation characteristics that are very different from those in lower frequency bands. The main features of the EHF band should thus be addressed in order to evaluate the realistic capabilities of mmWave communication systems in terms of channel impulse response and coverage radius dispersion, coherence time and bandwidth deviation, as well as reliability of coverage.

For the above reasons, a lot of studies are directed at obtaining statistics desirable for channel characterization. To date, ray-tracing (RT) based approaches remain the most popular in simulating wireless propagation in indoor and outdoor environments alike. Being an accurate tool, it however suffers from low efficiency when complicated deployments with multiple antennas and highly detailed environment are under consideration. A number of papers [5], [6], [7] are addressing how the exact scenario might be generated in the RT simulator.

The use of a building database and RT techniques for predicting the channel characteristics in microcell environments was proposed in [8]. These results were then validated with real measurements. These showed that the predicted values fall within 5 dB of the measured data. In [9], the real measurements of a mmWave communication system were conducted to obtain insights into the channel propagation characteristics as well as calibrate the RT-based simulations. It was shown that even for the more difficult non line-of-sight (nLoS) links, mmWave communication still operates satisfactorily. In addition, with the help of the RT tool, the propagation channel model for the mmWave systems was designed [10], [11].

Even though there are multiple papers describing the RT tools in order to quantify channel characteristics, the main limitation of the previous works is their focus on individual propagation environments. In the past, simplified models of real environments were used, since this reduces the overall simulation time. Various techniques were employed to speed up the simulations, such as a method of images applied in [6]. When the real experiment is conducted, it is even more complicated to consider multiple real deployments. Hence, it is common to have an experiment in a single area of interest and then consider a statistical propagation model. Indeed, it is a reasonable approximation for a scenario similar to the one that has been used in the experiment. However, those data may not be sufficient to yield conclusions on the propagation models within different scenarios. This is because the topology of the deployment in question directly impacts the performance results.

In this paper, we develop a methodology that makes it possible to collect statistical data from a large number of real scenarios given by their maps. Various statistics could be derived to obtain a deeper understanding on the mmWave propagation for the desired selection of scenarios. Moreover, our methodology is able to resolve the main challenges arising during the collection of a large number of statistical inputs needed for the channel modeling. As small cells in the EHF bands are expected to offer shorter coverage ranges in comparison to these in the lower frequency bands, it is important to have more transmitters (Tx) for resulting uninterrupted coverage. Providing reliable connectivity for system operators should also benefit the connection quality for the end users. Hence, the ability to model massive Tx locations in a single simulation run is essential to estimate the sufficient number and the desired placement options of multiple Tx. To this aim, we propose a 2D shoot-and-bounce ray (SBR) based methodology, which is specifically applicable for the task at hand.

The rest of this text is organized as follows. The description of the proposed methodology is provided in Section II. It includes the description of the automated base station placement method as well as the feature of our methodology named image-based SBR. We demonstrate preliminary simulation results in Section III. Conclusions and future work are highlighted in the last section.

II. Proposed Methodology

A. General description

The flowchart of the proposed methodology is provided in Fig. 1. As the first step, we generate a list of 2D maps and store it in the environment database. Each of the maps accurately repeats the detailed topology of real cities. As soon as the map is loaded into the database, the loop execution starts. It takes one of the ordered maps from the database and transfers it to the function, which translates the map into a Matlab structure. This structure comprises a geometric description of the environment objects in the 2D Cartesian coordinate system. There are additional fields in the structure with Tx and receiver (Rx) positions. These are predefined by the specialized base station placement algorithm described below. Further, the main step is shoot-and-bounce ray-tracing simulation, which characterizes electromagnetic propagation of multipath components (MPCs) based on the Maxwell equations. The main goal of the SBR method is to identify the channel impulse response (CIR) for each of the Tx-Rx pairs inside a given environment.

Our output results describe all of the possible Tx-Rx channels in time, power, and angular (in case of directionality) domains. From the implementation viewpoint, the SBR produces an array $N \times M$ where each N Tx correspond to M Rx describing the CIR. In this paper, we study a characteristic map with multiple antennas as a confirmation of applicability of our proposed methodology.

B. Map extraction and processing

Real maps of 2D buildings are extracted from the OpenStreetMap project as described in [12], [13]. Each building is represented by a simple polygon. The polygons are combined using the polygonal union operation, and their insides are removed. Hence, we are left with the street canyons where the electromagnetic waves are expected to propagate. Each of the polygons can be resolved in primitive environment objects, such as vertices and lines. The first object represents the corners of the buildings while lines play the role of walls.

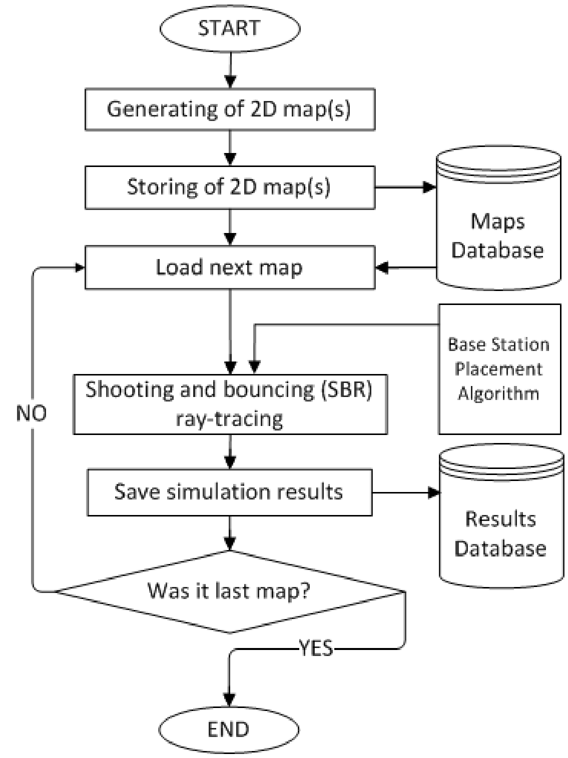

Fig. 1. Structure of the proposed methodology.

C. Automated base station placement algorithm

An algorithm for automatic search of appropriate locations for the base stations on the facades of the buildings is described in [13] and follows these main steps:

1) Once the buildings have been merged together, there is a clear outside perimeter for every city block. It is then possible to search around this perimeter for desirable wall-mounted base station locations.
2) Every block is connected to its natural neighbor[1] blocks by the shortest linking segment. The points of contact partition the contour of a block into several sections.
3) When each wall section is identified, the algorithm searches for the location that has the highest line-of-sight (LoS) area within the perimeter of 200 m.

D. Utilized SBR method

The key element of our proposed methodology is the image-based SBR method, which simulates propagation of the radio waves inside a certain scenario. Constituting a hybrid technique that integrates image-based RT and brute-force casting Ray-Launcher (RL), it removes all the inherent limitations

[1]Natural neighbors are defined based on the Generalized Voronoi Diagram (GVD) of the city blocks. Natural neighbor blocks are those whose GVD cells are touched.

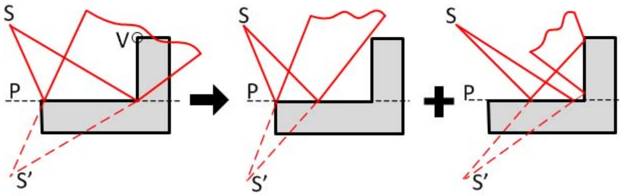

Fig. 2. Beam decomposition by the internal edge.

of both models. Based on our experience, we note that the key bottleneck of the classical RL is a finite-sized receiving sphere, which produces phase errors as well as suffers from the ”ray skipping” effect when the sphere's size is not large enough [6]. Despite the fact that the canonical image-based RT method is more accurate, it remains highly sensitive to the number of antennas and the scenario complexity [14]. Since the most attractive deployments for our aimed study may include hundreds of Tx and Rx within one highly detailed scenario, the usage of said tool might be challenging as it does not provide sufficient calculation speed.

To make the simulations faster, we reduce the space dimensionality from 3D to 2D. This shift is possible if we assume that multiple Tx and Rx are located on the same height, and the wave propagation occurs on a 2D plane (i.e., XY-plane). In addition, we also have to neglect the roof top diffraction and assume that all of our our antennas are positioned close to the ground. However, such implementation – due to the absence of the third coordinate (Z-axis) – has a limitation as it does not take into account the role of the ground reflected beams straightforwardly. To reduce the impact of these effects, we may emulate additional ”artificial” beams reflected from the ground. It can be done by using the elements of a so-called two-ray model [15], without any additional geometric simulations since these are the most expensive in terms of time consumption.

The geometric part of the 2D SBR is based on the following principle: it shoots the beams (triangles) from the Tx in all directions (in case of an isotropic radiator) and checks whether the objects are inside or not. Depending on the object type, which is occluded in the triangle, the three different phenomena may occur. If there is only Rx inside the triangle, then we have free-space loss between the Tx antenna and the Rx. As long as SBR occludes fully or partially a particular line, the reflection occurs in relation to the plane P as illustrated in Fig. 2 by using the source image S'. Diffraction can be observed when at least one vertice is located inside the triangle and effectively works as a new source of beams around it.

However, to make our geometric calculations more efficient, we also conduct preprocessing, where a visibility tree for every object in our scenario is constructed. To save memory consumption, we organize it such that every object is stored in the memory only once, but it can have access to other visible objects in the deployment. The combination of all the branches between the objects produces a visibility tree, where the Tx is located at the root node.

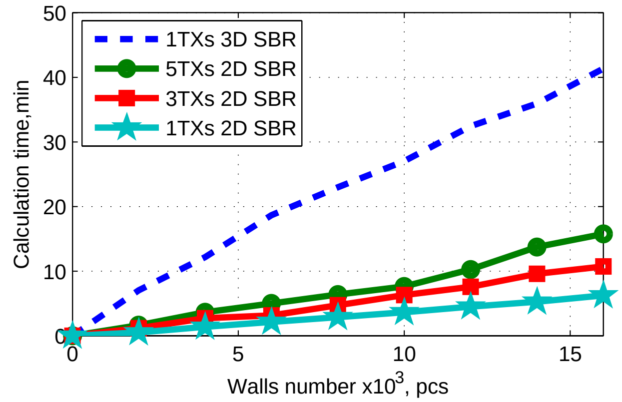

Fig. 3. Comparison of 3D SBR and 2D SBR in terms of simulation speed.

Based on our prior research, we report that the potential usage of beams represented by triangles is more efficient than utilization of lines used in RL tools [6]. However, the replacement of the wavefront representing said primitive brings more complexity to the implementation of the geometric part. For example, the beam decomposition as shown in Fig. 2 becomes a much more complicated task than the brute-force ray casting used in RL methods. Despite the fact that SBR ray-tracing is not a novel approach, and its basic principles were described in the literature previously [16], [17], [18], its algorithmic implementation is not detailed well in existing publications.

Our current implementation is based on a search of occluded vertices V within a triangle that makes the beam splitting, as summarized in Fig. 2. The number of produced beams is equal to the number of occluded vertices. The coordinates of the beam splitting are defined as a projection of the occluded vertices on the Tx through all the intermediate projections on the surfaces.

The physical part of our methodology is based on 2D geometric optics (GO) as well as the uniform theory of diffraction (UTD). Both these theories are well described in past literature [19], [20] and do not contribute significantly to the key novelty of this paper. However, it has to be mentioned that since we evaluate the mmWave bands – that suffer from diffuse scattering – an appropriate estimation for the coefficient of roughness should be adopted additionally.

III. Current Simulation Results

The geometric part of our implemented methodology consumes most of the simulation time for calculating the paths for each Tx-Rx pair. Hence, we begin with the first-order comparison between the following simulators: a commercially available 3D SBR and our current version of 2D SBR. Along these lines, we took into account the dependence between the computation time and the number of environment objects as well as the number of Tx. It is reported in Fig. 3 that 2D SBR operating with 5 Tx produces better results in terms of simulation time than 3D SBR with only a single Tx. These results are encouraging as they confirm that a translation from

3D to 2D significantly reduces the number of beams that have to be processed. Moreover, the 2D beam processing algorithm works faster and more straightforwardly. Given that our 2D SBR implementation is still in process of finalization, a further optimization of lower-level programming constructs may provide an additional reduction in computation time.

Further, we investigate the question of how much power might be lost on the Rx when working with 2D SBR with the propagation in XY-plane in relation to 3D SBR with the propagation in XYZ-space. Since our implementation of the 2D SBR is not fully complete as of yet and requires more research, this important question can be answered by using our full-fledged 3D version of RL developed previously. For this purpose, we first generate a 3D map of the real environment of Paris as shown in Fig. 4 and then place the Tx (red circles) as illustrated in Fig. 5 according to base station placement algorithm described above in subsection II-C.

In addition to the above, the Rx grid (gray square) has been added to the deployment with an equidistant step equal to 5 m. Since only outdoor scenarios are under consideration in our present study, the algorithm of Rx placement positions the Rx outside of the buildings. All of the antennas in our deployment are isotropic (uniform gain 1 dBi), while the Tx radiate power of 25 dBm, which is common for today's femtocell base stations. To emulate the 2D case in a 3D RL, we place all the antennas at the same height of 2 meters and convert the spherical isotropic radiator into a circular one by only considering rays located at the equator of the sphere.

The resulting calculated coverage map is demonstrated in Fig. 6. It reports the amount of power received by each of the Rx in the grid. All the beams in the output results that interact with the ground were removed as well. At the same time, to offer a feasible way of improving the overall accuracy in the 2D case, we add extra power to the LoS Rx by using the two-ray model elements. The result is displayed in Fig. 7 and it can be observed that the difference within the Rx group in the 3D case can vary from 2 to 6 dB comparing to the same Rx group in the 2D case. However, the additional ground reflected LoS paths (Rx group with the received power of > -68 dBm) make this difference negligibly small.

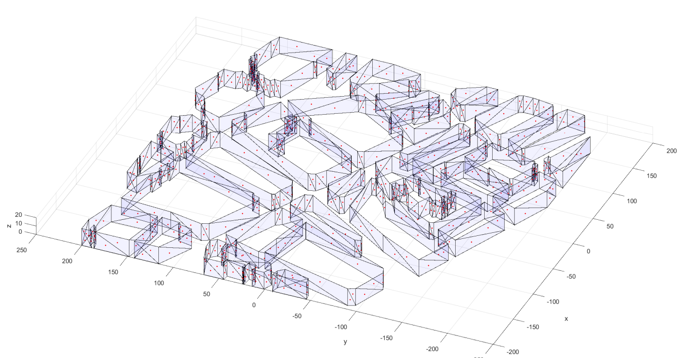

Fig. 4. Considered 3D model of Paris as an example.

Fig. 5. Top view of our target deployment.

IV. Conclusions and Future Work

Our study is focused on massive simulations represented by a large number of mmWave small cells located on a detailed square map of a real city. The proposed approach offers a better understanding of the EHF propagation properties comparing to past simulation results concentrating on a single map with a simplified deployment. Clearly, our target research poses a non-trivial challenge for the deterministic ray-based models since the RT and RL tools are very sensitive to the amount of input data, which depends on the deployment accuracy. In this paper, we make the first decisive step in the desired direction and propose a 2D SBR-based methodology that may potentially collect channel statistics across many realistic city maps in a reasonable time. Taking into account our reported first-order estimation of the needed computation time, we can expect 8 – 10 hrs of simulation time for 200 Tx inside such detailed scenario.

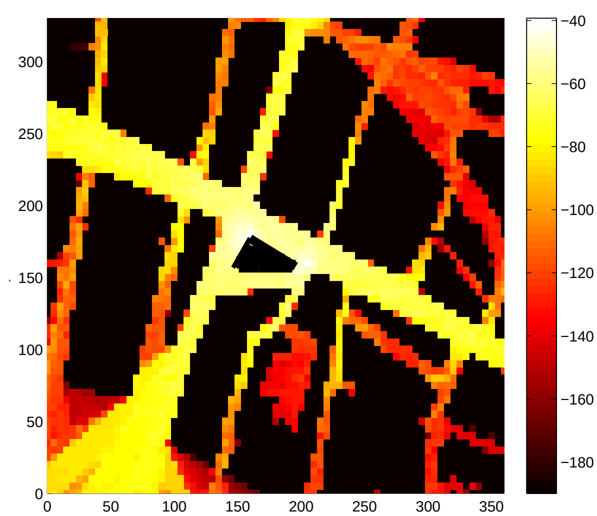

Fig. 6. Coverage map with our 2D SBR (Tx # = 5, radiated power 25 dBm).

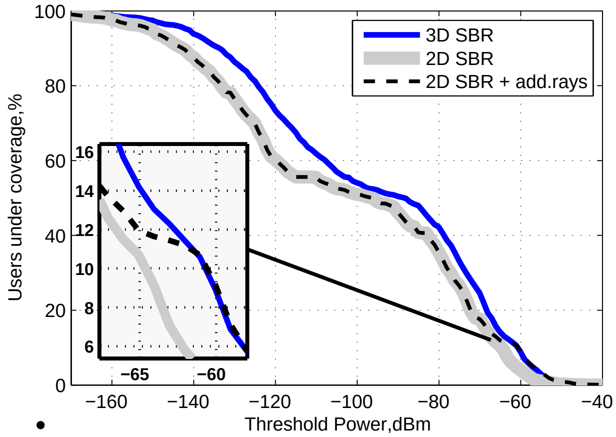

Fig. 7. Power loss at 2D SBR in relation to 3D case.

To further increase the resulting accuracy, additional rays reflected from the ground might be considered. Owing to their non-geometric nature, such rays will not take much extra simulation time. As our next step, we aim to complete the 2D SBR simulator and validate it with practical mmWave measurement results e.g., available in the literature. In addition, we may need to design methods that support directional antennas, which will become an important consideration in the future mmWave systems.

ACKNOWLEDGMENT

This work was supported in part by the Academy of Finland and in part by the project TT5G: Transmission Technologies for 5G.

REFERENCES

[1] J. Andrews, S. Buzzi, C. Wan, S. Hanly, A. Lozano, A. Soong, and J. Zhang, "What will 5G be?," *IEEE Journal on Selected Areas in Communications*, vol. 32, pp. 1065–1082, June 2014.

[2] A. Ghosh, T. Thomas, M. Cudak, R. Ratasuk, P. Moorut, F. Vook, T. Rappaport, G. MacCartney, S. Sun, and S. Nie, "Millimeter-wave enhanced local area systems: a high-data-rate approach for future wireless networks," *IEEE Journal on Selected Areas in Communications*, vol. 32, pp. 1152–1163, June 2014.

[3] M. Jacob, S. Priebe, T. Kurner, M. Peter, M. Wisotzki, R. Felbecker, and W. Keusgen, "Fundamental analyses of 60 GHz human blockage," in *7th European Conference on Antennas and Propagation (EuCAP)*, pp. 117–121, April 2013.

[4] S. Rangan, T. Rappaport, and E. Erkip, "Millimeter-wave cellular wireless networks: Potentials and challenges," *IEEE Proc.*, vol. 102, pp. 366–385, March 2014.

[5] M. Lott and B. Walke, "The indoor radio channel at 5.2 GHz: Prediction by means of ray tracing and measurements," *IEEE 55th Vehicular Technology Conference (VTC 1999 - Fall)*, vol. 4, pp. 2293–2297, September 1999.

[6] G. Durgin, N. Patwari, and T. Rappaport, "An advanced 3D ray launching method for wireless propagation prediction," *IEEE 47th Vehicular Technology Conference*, vol. 2, pp. 785–789, May 1997.

[7] J. Ling, D. Chizhik, and R. Valenzuela, "Predicting multi-element receive and transmit array capacity outdoors with ray tracing," *IEEE 53rd Vehicular Technology Conference*, vol. 1, pp. 392–394, May 2001.

[8] K. Schaubach, N. Davis, and T. Rappaport, "A ray tracing method for predicting path loss and delay spread in microcellular environments," *IEEE 42nd Vehicular Technology Conference*, vol. 2, pp. 932–935, May 1992.

[9] M. R. Akdeniz, Y. Liu, M. K. Samimi, S. Sun, S. Rangan, T. S. Rappaport, and E. Erkip, "Millimeter wave channel modeling and cellular capacity evaluation," *IEEE Journal on Selected Areas in Communications*, vol. 32, pp. 1164–1179, June 2014.

[10] S. Baek, Y. Chang, S. Hur, J. Hwang, and B. Kim, "3-Dimensional large-scale channel model for urban environments in mmWave frequency," in *IEEE International Conference on Communication Workshop (ICCW)*, June 2015.

[11] S. Hur, S. Baek, B. Kim, J. Park, A. F. Molisch, K. Haneda, and M. Peter, "28 GHz channel modeling using 3D ray-tracing in urban environments," in *9th European Conference on Antennas and Propagation (EuCAP)*, May 2015.

[12] M. Mirahsan, R. Schoenen, S. S. Szyszkowicz, and H. Yanikomeroglu, "Spatial heterogeneity of users in wireless cellular networks based on open urban maps," in *IEEE ICC*, June 2015.

[13] S. S. Szyszkowicz, A. Lou, and H. Yanikomeroglu, "Automated placement of individual millimeter-wave wall-mounted base stations for line-of-sight coverage of outdoor urban areas," in *IEEE Wirel. Commun. Letters*.

[14] N. Bessis, *Development of Distributed Systems from Design to Application and Maintenance*. IGI Global, 1 ed., December 2012.

[15] R. Aquino-Santos, *Wireless Technologies in Vehicular Ad Hoc Networks: Present and Future Challenges*. IGI Global, 2012.

[16] H. S. Sato and K. Otoi, "Electromagnetic wave propagation estimation by 3-D SBR method," *Electromagnetics in Advanced Applications, ICEAA*, pp. 129–132, 2007.

[17] S. H. Chen, "An SBR/image approach for radio wave propogation in indoor environments with metallic furniture," *IEEE Transactions an Antennas and Propogation*, vol. 1, no. 45, pp. 98–106, 1997.

[18] S. Chen and S. K. Jeng, "SBR image approach for radio propagation in tunnels with and witwith traffic," *IEEE Transactions on Antennas and Propagation*, vol. 3, no. 45, pp. 570–578, 1996.

[19] D. McNamara, C. Pistotius, and J. Malherbe, *Introduction to the Uniform Geometrical Theory of Diffraction*. Artech House, 1990.

[20] F. S. de Adana, O. G. Blanco, I. G. Diego, J. P. Arriaga, and M. F. Catedra, "Propagation model based on ray tracing for the design of personal communication systems in indoor environments," *IEEE Transactions on Vehicular Technology*, vol. 49, pp. 2105–2112, November 2000.